A system model for investigating passive electrical properties of neurons

A. D'Aguanno,*§¶ B. L. Bardakjian,*§‖ and P. L. Carlen‡‖¶

Departments of *Electrical Engineering, ‡Physiology, ‡Medicine (Neurology), §Institute of Biomedical Engineering, ‖Playfair Neuroscience Unit, Toronto Western Hospital, ¶Addiction Research Foundation, University of Toronto, Toronto, Ontario, Canada

ABSTRACT Passive membrane properties of neurons, characterized by a linear voltage response to constant current stimulation, were investigated by busing a system model approach. This approach utilizes the derived expression for the input impedance of a network, which simulates the passive properties of neurons, to correlate measured intracellular recordings with the response of network models. In this study, the input impedances of different network configurations and of dentate granule neurons, were derived as a function of the network elements and were validated with computer simulations. The parameters of the system model, which are the values of the network elements, were estimated using an optimization strategy. The system model provides for better estimation of the network elements than the previously described signal model, due to its explicit nature. In contrast, the signal model is an implicit function of the network elements which requires intermediate steps to estimate some of the passive properties.

I. INTRODUCTION

Passive electrical properties of neuronal membranes have been investigated using network models. A commonly used network model is the passive lumped somatic-dendritic cable model (Fig. 1 a), initially developed by Rall (30–32), and since used by many others (2–10, 17–19, 21, 22, 38, 39). Other network models have also been used (11, 25–28, 33, 36). Analysis of Rall's cable model has taken the form of expressing the voltage along the dendritic cable as a partial differential equation (30–32). Solving the equation for a current impulse produces a characterizing voltage response. The response, henceforth defined to be the signal model, is expressed as a summation of exponential terms with decreasing time constants. Each exponential term is characterized by an amplitude coefficient and a time constant; no restrictions are placed upon the number of exponential terms that constitute the response (30). Extracting the signal model parameters from the voltage response allows some of the membrane parameters (i.e., input resistance, membrane time constant, somatic capacitance, electrotonic length) to be characterized by evaluating prederived expressions (10, 30). Some of the many steps involved with the signal model approach suffer from accuracy problems (7, 32) which restrict the full utilization of the signal model. These intermediate steps are avoided by the system model approach.

A system model approach in which the input impedance is expressed as an explicit function of the network elements can overcome some of the difficulties encountered by the signal model. A system model can be derived by using network analysis and z-transformation techniques (15, 16, 34). These techniques are applied to finite ladder networks composed of lumped elements. Hence the dendritic cable in the Rall model was replaced by an equivalent ladder network containing N finite compartments (25) (Fig. 1 b). The resulting system model expresses the input impedance as an explicit function of model elements and the number of ladder compartments. For the derivations to follow, the extracellular resistivity is assumed to be zero.

In this paper, system models are derived for a number of network configurations, with a special emphasis on uniform ladder networks. Increased network complexity, such as an eccentrically placed soma (multiple ladders) is also briefly covered.

II. METHODS

Biological data

Young mature adult male Wistar rats (150–200 g) were anesthetized with halothane and decapitated. The brain was rapidly removed (in <3 min) and placed in an ice cold artificial cerebrospinal fluid (ACSF) solution which contained (in millimolar) Na^+ 154, K^+ 3.25, Ca^{2+} 2.0, Mg^{2+} 2.0, Cl^- 131.5, HCO_3^- 26, $H2PO_4^{-2}$ 1.25, $H_2SO_4^{-2}$ 2.0, and dextrose 10. The hippocampus was dissected out and 300-μm slices were prepared with a microtome-based tissue chopper (Lancer Series 1000, Ted Pella Inc., Tustin, CA). The slices were then transferred into a holding chamber filled with oxygenated ice cold ACSF. The temperature in the holding chamber was gradually raised to 30°C. Intracellular recordings (glass microelectrodes, 3 M potassium acetate, 100–150 MΩ) were done in the recording chamber of a modified interface-type Haas bath. The slices were bathed with warm (34°C) oxygenated ACSF perfusing at a rate of 0.5–0.8 ml/min into the recording chamber.

0006-3495/89/06/1169/14 $2.00

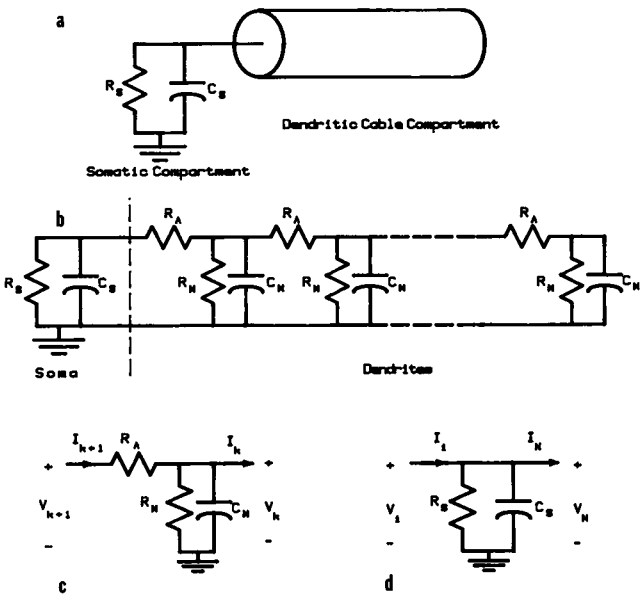

FIGURE 1 (*a*) The Rall network model contains a RC network simulating the somatic properties, and a uniform cable to simulate the dendritic properties of the neuron. The cable is characterized by an axial resistance per unit length, a membrane resistance per unit length, and a membrane capacitance per unit length of the cable. (*b*) The network consists of N finite compartments which simulates the cable in the Rall model. (*c*) A dendritic compartment for the system model. (*d*) The somatic compartment. V_i and I_i are voltage and current at the input terminals. V_N and I_N are voltage and current at the soma-dendrite interface.

The intracellular current injection and voltage recording were obtained with a single electrode in the soma and a grounding electrode in the ACSF solution. The electrode exhibited resistive and capacitive properties. Together, they resulted in an electrode time constant on the order of 0.1 ms which provided a limit for recording the fast responses. To ensure that none of the data selected for analysis were contaminated by the properties of the electrodes, all data within 1 ms after the onset of the stimulus were rejected. Passive properties of hippocampal dentate granule neurons were characterized by the voltage responses which were elicited every 4 s by short current pulses (0.5 ms, 5.0 nA). Upon completion of the experiments, the electrode characteristics were examined in the extracellular fluid. Recordings were only used from neurons with $R_{IN} > 40$ MΩ and spike heights > 80 mV.

Measured voltage responses and current stimuli were recorded on a Racal FM tape recorder. The voltage response was subsequently replayed, amplified, and lowpass filtered at a cutoff frequency which was 1/3 of the 10 KHz sampling frequency before being digitized. The neuron's characterizing response was formed by an ensemble average of eight individual responses selected from 10 recorded responses. Rejected responses were those with superimposed spontaneous potentials or timing artifacts. Voltage responses, each having a duration of 50 ms, were used for estimating the signal model parameters by an optimization strategy (7). The frequency spectra of the short pulse voltage decays (4,096 time-samples) were obtained via a Fourier Transform method (3) in which the integral was evaluated numerically using Simpson's Rule (26).

Computer simulations

Spice, running on an IBM AT (PSPICE version 2.1), is a numerical analysis program used for examining and simulating properties of electrical circuits. Values for the model parameters were chosen to be in the same range as reported physiological data (8). Then the program SPICE was used to simulate various network configurations (35) to check the validity of the derived input impedance expressions.

The derived mathematical expressions for the input impedances and their corresponding gradients were evaluated by computer programs. The spectra of the time domain voltage responses were obtained by evaluating the Fourier transform integral (1, 24, 29) using Simpson's rule for numerical integration (20).

Computer-aided parameter estimation

Using biological data from animal models or simulated data from computer models, the system model parameters were estimated using an optimization strategy in conjunction with a gradient method for function minimization (the Fletcher method [12–14]).

III. INPUT IMPEDANCE OF A SYSTEM MODEL

Dendritic compartments

The dendritic cable in the Rall model (30–32) is replaced by a ladder network consisting of identical compartments cascaded together. Rall has also taken this approach by replacing a single dendritic cable with multiple cable compartments (33). In our derivation, the ladder consists of N finite compartments with the 1st node located at the distal end, and the Nth node connected to the soma.

At the $(k + 1)$th node, the nodal voltage and current are a function of the previous (kth) nodal voltage and current and the compartment elements (Fig. 1 *c*).

The relationship between any two adjacent nodes are

$$V_{k+1} = [1 + R_A(G_M + sC_M)]\,V_k + R_A I_k \qquad (1)$$

and

$$I_{k+1} = (G_M + sC_M)\,V_k + I_k. \qquad (2)$$

R_A is the axial resistance per compartment, G_M is the membrane conductance per compartment, and C_M is the membrane capacitance per compartment. V_k is the complex voltage spectrum at the kth node, I_k is the complex current spectrum at the kth node, and s is the complex frequency variable (the Laplace variable).

Expressing the relationships in a matrix format,

$$\begin{bmatrix} V_{k+1} \\ I_{k+1} \end{bmatrix} = \begin{bmatrix} 1 + R_A(G_M + sC_M) & R_A \\ G_M + sC_M & 1 \end{bmatrix} \begin{bmatrix} V_k \\ I_k \end{bmatrix}. \qquad (3a)$$

This can be written as a matrix equation.

$$\mathbf{W}_{k+1} = H\,\mathbf{W}_k. \qquad (3b)$$

H is the hybrid matrix, and the vector $\mathbf{W}$ specifies the nodal voltage and current. Applying z-transforms spatially (34), a solution to the system of equations can be obtained. The transformed matrix equation becomes space dependent,

$$z\mathbf{W}(z) - z\mathbf{W}_0 = H\mathbf{W}(z) \tag{4a}$$

or

$$\mathbf{W}(z) = [zI - H]^{-1} z\mathbf{W}_0. \tag{4b}$$

Where $\mathbf{W}(z)$ is the z-transform of $\mathbf{W}_k$, and is the nodal voltage and current at the far end of the ladder,

$$\mathbf{W}_0 = \begin{bmatrix} V_0 \\ I_0 \end{bmatrix}. \tag{5}$$

Eq. 4b is solved by standard linear algebra techniques for matrix inversion (37).

$$\mathbf{W}(z) = \begin{bmatrix} \dfrac{z(z-1)}{(z-p)(z-q)} & \dfrac{zR_A}{(z-p)(z-q)} \\ \dfrac{z(G_M + sC_M)}{(z-p)(z-q)} & \dfrac{z[z - 1 - R_A(G_M + sC_M)]}{(z-p)(z-q)} \end{bmatrix} \cdot \begin{bmatrix} V_0 \\ I_0 \end{bmatrix}, \tag{6}$$

where $p = 1 + \frac{1}{2}(R_A)(G_M + sC_M) + \frac{1}{2}[(R_A)^2 (G_M + sC_M)^2 + 4R_A (G_M + sC_M)]^{1/2}$ and $q = 1 + \frac{1}{2}(R_A)(G_M + sC_M) - \frac{1}{2}[(R_A)^2 (G_M + sC_M)^2 + 4R_A (G_M + sC_M)]^{1/2}$. Notice that the roots in the denominator of Eq. 6 are eigenvalues of the H matrix. This was expected because other methods for solving systems of equations are based on matrix decomposition into eigen-value and eigen-vector format (37).

Applying the condition that no current leaves the network at the far end ($I_0 = 0$) reduces the corresponding solution vector, initially a product of a 2 × 2 matrix and a 2 × 1 vector, to a 2 × 1 vector with a scalar constant. Taking the inverse z-transform using the method of residues (20) gives the following expression for the voltage and current at the input of a cascaded ladder.

$$\mathbf{W}_N = \frac{V_0}{(p-q)} \begin{bmatrix} p^{N+1} - q^{N+1} - p^N + q^N \\ (p^N - q^N)(G_M + sC_M) \end{bmatrix}. \tag{7}$$

Somatic compartment

The somatic properties of a neuron are modeled by a parallel RC network. This network and the dendritic ladder network are arranged in a parallel configuration. The voltage and current at the input terminals can be related to the voltage and current at the Nth node of the dendritic compartments (Fig. 1 *d*).

$$V_i = V_N \tag{8}$$

and

$$I_i = V_N[G_S + sC_S] + I_N. \tag{9}$$

G_S is the somatic compartment membrane conductance, and C_S is the somatic compartment membrane capacitance. V_i is the complex voltage spectrum at the soma, and I_i is the complex current spectrum at the soma.

Expressing Eqs. 8 and 9 in a matrix format,

$$\mathbf{W}_i = \begin{bmatrix} 1 & 0 \\ G_S + sC_S & 1 \end{bmatrix} \mathbf{W}_N. \tag{10}$$

Substituting Eq. 7 into Eq. 10 allows the input voltage and current to the entire network to be expressed as follows,

$$\begin{bmatrix} V_i \\ I_i \end{bmatrix} = \frac{V_0}{(p-q)} \cdot \begin{bmatrix} p^{N+1} - q^{N+1} - p^N + q^N \\ (p^{N+1} - q^{N+1})(G_S + sC_S) - (p^N - q^N)[G_S - G_M) + s(C_S - C_M)] \end{bmatrix}. \tag{11}$$

The input impedance Z_i is, by definition, the complex voltage spectrum V_i divided by the complex current spectrum I_i at the input terminals (16). Hence,

$$Z_i = \frac{p^{N+1} - q^{N+1} - p^N + q^N}{(p^{N+1} - q^{N+1})(G_S + sC_S) - [p^N - q^N][(G_S - G_M) + s(C_S - C_M)]} \tag{12}$$

It is to be noted that (*a*) The complex spectrum can be evaluated on the imaginary axis of the complex frequency s plane using Fourier transforms (20). (*b*) Although q is the square root of a complex argument, no q term is raised to an odd power (binomial expansion theory); hence only real polynomial coefficients are observed. (*c*) The input impedance expression is an explicit function of all five network elements (G_S, C_S, R_A, G_M, and C_M) and the number of cascade compartments N in the dendritic component.

The system model parameters are related to the specific membrane parameters (for a spherical soma and an equivalent dendritic cylinder) as follows:

$$R_M = 1/G_M = R_{md}/[(2\pi a l_c)(1 + \tau)] \tag{13a}$$

$$C_M = C_{md}[(2\pi a l_c)(1 + \tau)] \tag{13b}$$

$$R_A = R_i(l_c)/\pi a^2 \tag{13c}$$

$$R_S = 1/G_S = R_{ms}/A_s \tag{13d}$$

$$C_S = C_{ms}(A_s) \tag{13e}$$

$$l_c = l_d/N, \tag{13f}$$

where

R_{md} is the dendritic membrane resistivity (Ω cm^2),

R_{ms} is the somatic membrane resistivity (Ω cm^2),

R_i is the specific cytoplasmic resistivity (Ω cm),

C_{md} is the specific dendritic membrane capacitance (μF/cm^2),

C_{ms} is the specific somatic membrane capacitance (μF/cm^2),

τ is a correction factor to account for the increase in dendritic surface area caused by the presence of dendritic spines,

l_d is the length of the dendritic cable (μm),

l_c is the length of each compartment,

A_s is the surface area of the soma (μm^2),

a is the equivalent cylinder radius (μm).

IV. PARAMETER ESTIMATION USING AN OPTIMIZATION STRATEGY

To use a numerical optimization strategy to estimate the model parameters, it is desirable to express the system model in terms of a real-valued approximating function. Hence, the square of the magnitude of the input impedance is chosen to represent the approximating function F_A of the system.

$$F_A(w) = |Z_i(jw)|^2. \tag{14}$$

The magnitude of the neuron's input impedance is obtained from the biologically measured voltage response to a short current pulse. The Fourier transform is applied to (a) the voltage response to obtain the magnitude of the voltage spectrum $|V_b(jw)|$, and (b) the input current to obtain the magnitude of the current spectrum $|I_b(jw)|$. The square of the magnitude of the neuron's biologically measured input impedance is chosen to represent the specified function F_S of the neuron.

$$F_S(w) = \frac{|V_b(jw)|^2}{|I_b(jw)|^2}. \tag{15}$$

A measure of the difference between the approximating function F_A and the specified function F_S is formulated as a least square objective function F_O which is to be numerically minimized to estimate the system model parameters (12–14).

$$F_O(G_S, C_S, R_A, G_M, C_M, w) = E_m \left\{ \sum_{n=1}^{NP} \left[\frac{F_A(n) - F_S(n)}{E_m} \right]^2 \right\}^{1/2}, \tag{16}$$

where $F_A(n)$ is the sampled approximating function, $F_S(n)$ is the sampled specified function, n is the sampling index, NP is the number of points in the approximation band, and E_m is the maximum error between the specified function and the approximating function.

$$E_m = \max_n [F_A(n) - F_S(n)]$$

The numerical minimization of the objective function is carried out using the Fletcher method (12–14). This is a gradient method for function minimization which requires the gradient vector of the objective function.

$$\nabla F_O = \frac{\sum_{n=1}^{NP} \left[\frac{F_A(n) - F_S(n)}{E_m} \right] \nabla F_A(n)}{(F_O)^{1/2}}, \tag{17}$$

where $\nabla F_A(n)$ is the sampled gradient of the approximating function.

To represent the physical system, and to ensure proper convergence, the optimization problem is constrained by the following parameter constraints: (a) All parameters of the approximating function should have positive values at all times. (b) All parameters should be scaled to avoid numerical ill conditioning. The parameter transformations can be written as

$$\mu_1(d_1)^2 = G_S \tag{18a}$$

$$\mu_2(d_2)^2 = C_S \tag{18b}$$

$$\mu_3(d_3)^2 = R_A \tag{18c}$$

$$\mu_4(d_4)^2 = G_M \tag{18d}$$

$$\mu_5(d_5)^2 = C_M. \tag{18e}$$

where $(d_1, \ldots, d_5)$ are the unconstrained parameters and $(\mu_1, \ldots, \mu_5)$ are the scale factors. (c) The maximum error E_m is a scalar used in the formulation of the objective function, to normalize the number raised to the power 2 to be <1. This helps to reduce numerical difficulties and ill conditioning in the objective function.

The gradient of the approximating function with respect to the model parameters is given in Appendix I.

RESULTS

Three cases were used to elucidate the system model approach for investigating the passive electrical properties of neurons. The first case dealt with a computer model of a neuron with uniform dendritic compartments whereby the following questions were considered: (a) What number of compartments was adequate to represent the dendritic cable for dentate granuel neurons? (b) Was the derived expression for the input impedance (Eq. 12) valid? (c) Which model parameters, if any, had the

strongest influence on the input impedance? (*d*) Was the proposed optimization strategy for estimating the system model parameters a valid approach? The second case dealt with the issue of increased complexity of the model structure. For example, two uniform ladders having different numbers of compartments were used to represent two dendritic cables having different lengths, and connected to the soma. Computer models were used to demonstrate the effect of an eccentrically placed soma on the magnitude of the input impedance. Finally, the third case dealt with the application of the system model approach to biological data. The system model approach was compared with the signal model approach to establish the validity of the system model approach.

Case 1: a neuron with uniform dendritic compartments

(*A*) The effect of the number of dendritic compartments on the magnitude of the input impedance was investigated by dividing the finite cable (Fig. 1 *a*) into smaller equivalent cylinders and approximating each small cylinder by an RC ladder compartment (Fig. 1 *b*). Each ladder compartment consisted of resistances and capacitances (Fig. 1 *c*) which were computed (using Eq. 13, a–e) from the following mean biological data of dentate granule neurons (8).

$R_{md} = 6632\,\Omega\,cm^2$, $R_{ms} = 1010\,\Omega\,cm^2$, $R_i = 173.4\,\Omega\,cm$,
$C_{md} = 4.48\,\mu F/cm^2$, $C_{ms} = 4.48\,\mu F/cm^2$, $\tau = 0.6$,
$l_d = 287\,\mu m$, $A_s = 470\,\mu m^2$, and $a = 1.2\,\mu m$.

The values of the resistances and capacitances are given in Table 1 where the specific membrane resistances and capacitances were kept constant but the number of compartments was varied. Fig. 2 demonstrates that as the number of compartments N was increased, the magnitude of the input impedance became less dependent upon N. Also, 20 ladder compartments were adequate to approximate the finite cable because the magnitude of the input impedance for 15 and 20 ladder compartments were almost identical. Furthermore, using 100 compartments, the magnitude of the input impedance was still identical to that for 20 compartments.

(*B*) The validity of the derived expression for the input impedance was checked by considering an RC ladder network as in Fig. 1 *b*, having the following parameters: $R_A = 10$ MΩ, $R_S = 100$ MΩ, $C_S = 25$ pF, $R_M = 250$ MΩ, $C_M = 100$ pF, and $N = 20$.

The magnitude of the input impedance was computed using (*a*) Spice simulation of the network model, and (*b*) the derived expression for the input impedance (Eq. 12). The mean square error between the above two computed magnitudes of the input impedance was 0.00025 $M\Omega^2$. This demonstrated that the derived expression for the input impedance was valid.

(*c*) The relative importance of the parameters of the system model was investigated by computing the gradient and the sensitivity of $|Z_i|^2$ with respect to the network elements (Appendix I). The magnitude of the gradient and the magnitude of the sensitivity of $|Z_i|^2$ with respect to the network elements, for the RC ladder network of case 1B, are depicted in Fig. 3, *a* and *b*, respectively. The relative importance of the model parameters was more evident from the magnitude of the sensitivities which consider relative changes in parameter values, because the absolute parameter values varied dramatically ($\sim 10^{-11}$ to 10^7).

The magnitude of the input impedance was most sensitive to changes in R_A at higher frequencies and to changes in G_S at lower frequencies (Fig. 3 *b*). There were two critical frequencies (~50 and 400 Hz) such that the magnitude of the input impedance was not changed by changes in (*a*) G_M at the lower critical frequency, and (*b*) C_M at the higher critical frequency (Fig. 3 *a*).

(*D*) The validity of the parameter estimation technique was checked as follows. (*a*) A network model having 20 RC ladder compartments (Fig. 1 *b*) with a priori known model parameters given as the "true values" in Table 2, was simulated using Spice. (*b*) The squared magnitude of the input impedance was obtained from the Spice simulation, and was used as the specified function in the optimization strategy (section IV). (*c*) The squared magnitude of the input impedance was obtained from Eq. 12 for 20 compartments, and was used as the approximating

TABLE 1 Effect of number of dendritic compartments on system model parameters

No. compartments	1	2	3	5	10	15	20
R_S ($M\Omega$)	214.9	214.9	214.9	214.9	214.9	214.9	214.9
C_S (pF)	21.06	21.06	21.06	21.06	21.06	21.06	21.06
R_A ($M\Omega$)	109.1	54.55	36.37	21.82	10.91	7.273	5.455
R_M ($G\Omega$)	0.19	0.38	0.57	0.95	1.9	2.9	3.8
C_M (pF)	155.8	77.88	51.92	31.15	15.57	10.38	7.79
l_c (μm)	287	143.5	95.66	57.4	28.7	19.13	14.35

The finite cable was divided into RC ladder compartments without changing the specific membrane resistances and capacitances.

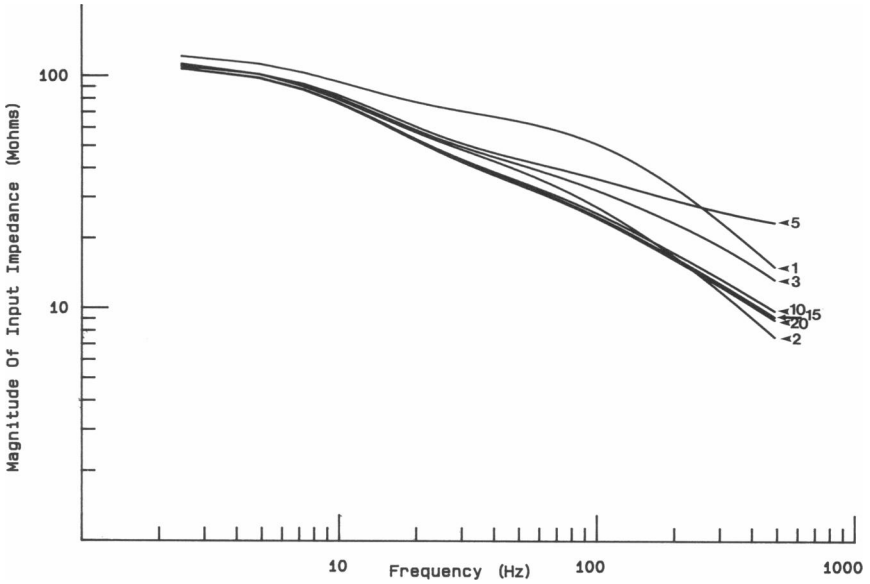

FIGURE 2 The magnitude of the input impedance using 1, 2, 3, 5, 10, 15, and 20 dendritic compartments, respectively.

function. (*d*) The minimization of the objective function (Eq. 15) was started using two different starting parameter values, (2, 2, 2, 2, 2) and (7, 7, 7, 7, 7). (*e*) The final parameter values at a locally optimal solution were compared with their a priori known true values.

The optimization strategy converged to a locally optimal solution, given as the estimated values in Table 2. The objective function value at the locally optimal solution was 0.1 $M\Omega^2$, which corresponds to a mean square error of 0.01 $M\Omega^4$ between the estimated and true squared magnitude of the input impedance. The error in the parameter estimates was <0.2%.

Case 2: a neuron with an eccentrically placed soma

The expression for the input impedance of a neuron with an eccentrically placed soma and 20 dendritic compartments is derived in Appendix II. Such a model structure could represent, for example, CA_1 neurons which have two dendritic trees, a long apical tree and a shorter basilar tree. To simulate such a structure, two uniform RC ladders having 15 and 5 compartments, respectively, were used to represnt two dendritic cables having different lengths, and connected to the soma (Fig. 4 *a*).

Two model structures were considered, the first having an eccentrically placed soma (Fig. 4 *a*), and the second having a terminally placed soma (Fig. 1 *b*). The following parameters were used for both structures: R_A = 10 MΩ, R_S = 100 MΩ, C_S = 25 pF, R_M = 250 MΩ, and C_M = 100 pF. The magnitude of the input impedance for both model structures is depicted in Fig. 4 *b*, where the effect of an eccentrically placed soma was to lower the magnitude of the input impedance.

TABLE 2 Validation of parameter estimation using the system model

Parameter	Estimated value	True value	Percentage difference
G_S (nS)	10.005	10.000	0.1
C_S (pF)	24.970	25.000	0.1
R_A ($M\Omega$)	9.992	10.000	0.1
G_M (nS)	3.992	4.000	0.2
C_M (pF)	99.860	100.000	0.1

True values were used to simulate a circuit model. Estimated values were obtained from the optimization strategy.

Case 3: biological data from dentate granule neurons

The signal and system model parameters were estimated from a measured voltage response (Fig. 5 *a*) to a short hyperpolarizing current pulse (5 nA, 0.5 ms). The signal model parameters for a voltage response represented by a summation of four exponential terms were estimated using an optimization strategy described elsewhere (7), and are given in Table 3. The system model parameters for N = 20 were estimated as described in section IV, and are given in Table 4. The resistances and capacitances of the RC ladder structure were also estimated from the

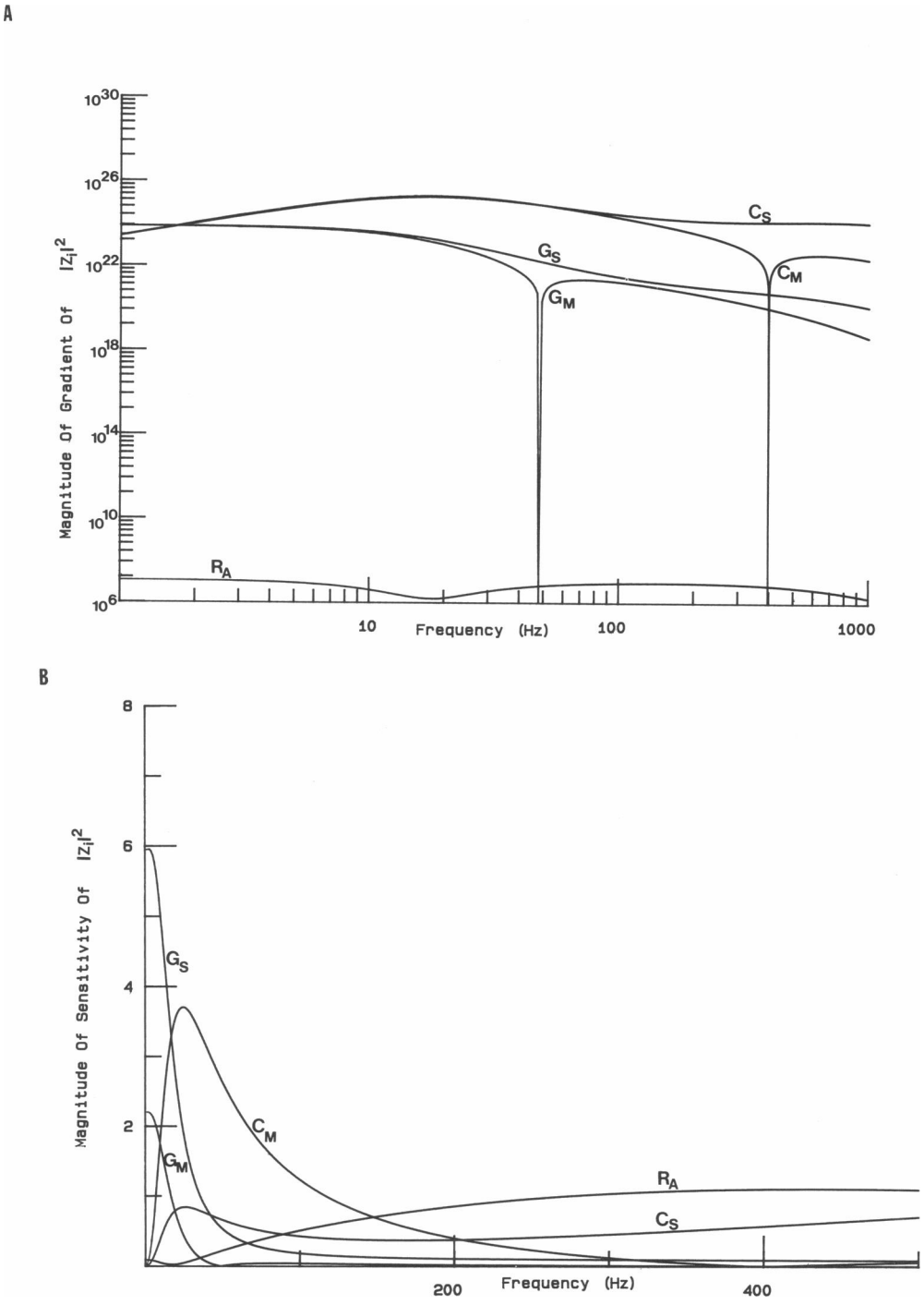

FIGURE 3 The magnitude of (*A*) the gradient and (*B*) the sensitivity of $|Z_i|^2$ with respect to the network elements (G_S, C_S, R_A, G_M, C_M). These are computed for an RC ladder network having the following parameters: R_A = 10 MΩ, R_S = 100 MΩ, C_S = 25 pF, R_M = 250 MΩ, C_M = 100 pF, and N = 20.

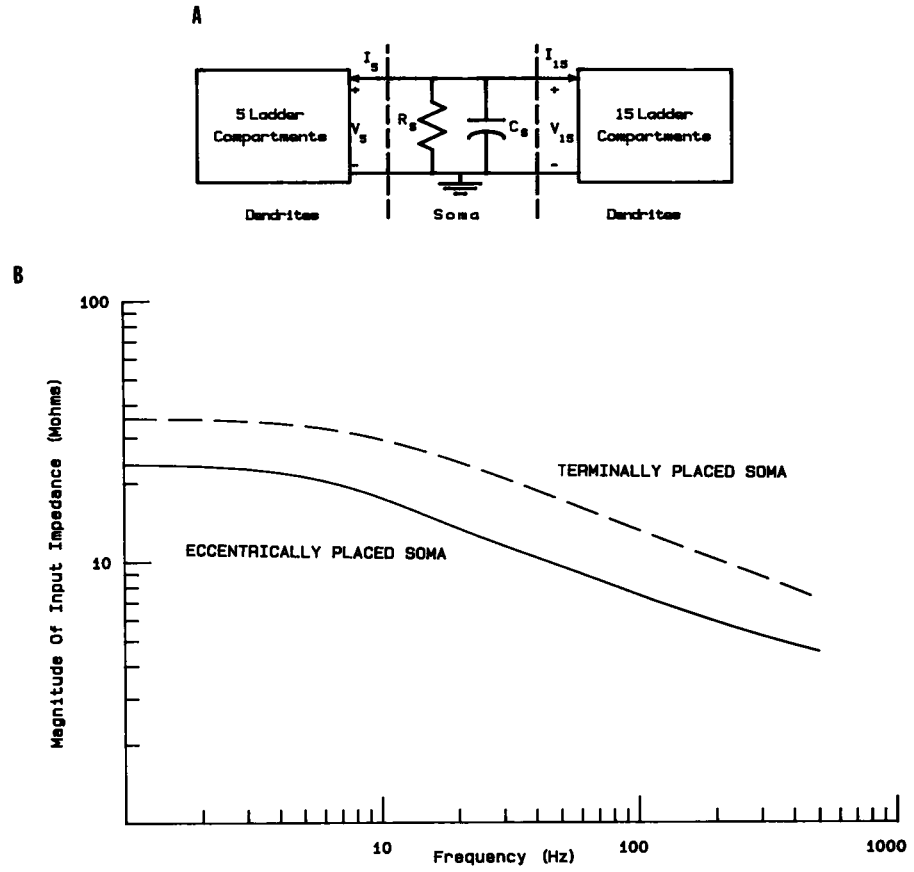

FIGURE 4 (*A*) Configuration for a neuron with an eccentrically placed soma and 20 dendritic compartments. (*B*) Magnitude of the input impedance for an eccentrically placed soma (*solid line*) and for a neuron with a 20 compartment dendritic tree and the soma at the end of the dendritic cable (*dashed line*). Input impedances of all models are measured from the soma.

signal model parameters, as described elsewhere (9) and in Appendix III; these values are given in Table 4.

The input resistance was estimated to be 94.9 MΩ from the signal model and 93.5 MΩ from the system model. Table 5 gives the specific membrane resistances and capacitances obtained from (*a*) the system model using the mean anatomical measurements outlined in case 1 (8), and (*b*) the signal model mean estimates as reported in reference 8. The estimated and measured voltage responses from the signal and system models are shown in Fig. 5 *b* and *c*, respectively, whereas for the system model, the measured and estimated magnitude of the input impedance are shown in Fig. 5 *d*.

VI. DISCUSSION

The system model approach for investigating the passive electrical properties of neurons, is characterized by an analytical expression for the input impedance of a one port network of resistances and capacitances. An RC ladder network is chosen to represent the dendritic cable, rather than parallel RC compartments (23, 40), to allow for the inclusion of axial components in the model structure. This approach can be used to investigate neurons that can be represented by a soma and a uniform dendritic cable (for example, dentate granule neurons) or a soma and two dendritic cables having different lengths (for example, CA1 neurons). This suggests the suitability of the system model approach to deal with increased complexity of the model structure.

A computer model of a neuron with uniform dendritic components demonstrated that (*a*) the derived analytical expression for the input impedance is valid. (*b*) When the number of compartments was varied, it was observed that, for dentate granule neurons, 20 compartments were adequate to represent the dendritic cable. This observation is only valid for dentate granule neurons and cannot be generalized to other neurons. (*c*) There are two critical frequencies such that small changes in G_M (at the lower critical frequency) and C_M (at the higher critical frequency) will cause no change in the magnitude of the input

impedance. The relevance of the two critical frequencies has to be clarified in the biological system. (*d*) The magnitude of the input impedance was most sensitive to changes in R_A at higher frequencies. One would not have predicted that the axial resistivity is the most sensitive element in the model at higher frequencies. This observation requires further investigation and it could change our view of the role of the dendritic cytoplasm. Axial resistances have played a relatively minor role to date when neuronal cable properties are studied. (*e*) The proposed

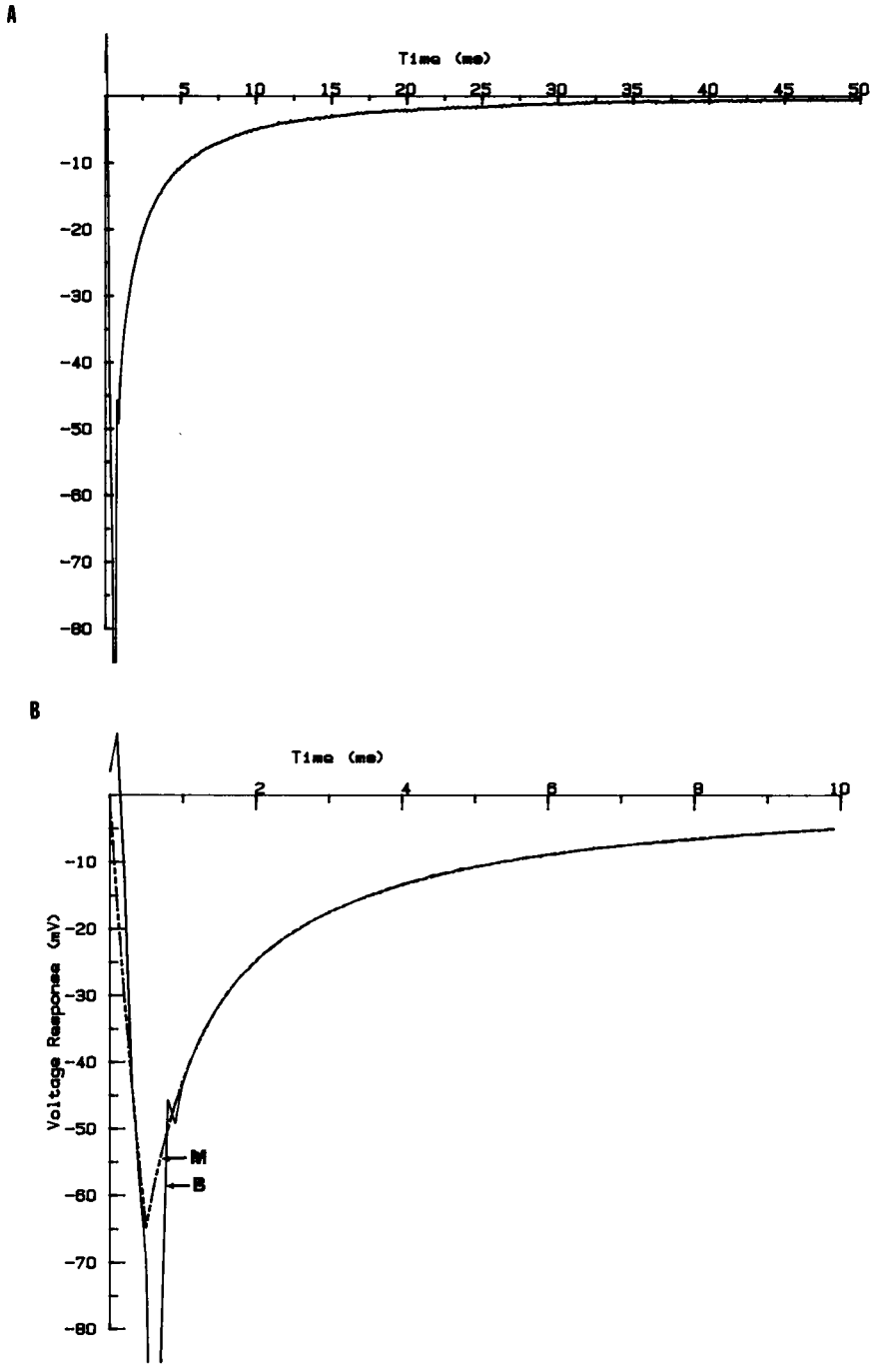

FIGURE 5 Biological data from a dentate granule neuron. (*A*) Voltage response to a short current pulse. (*B*) Model (*M*) and biological (*B*) voltage responses using the signal model. Note the shorter time base. (*C*) Model (*M*) and biological (*B*) voltage responses using the system model. (*D*) $|Z_1|^2$ of model (*M*) and biological (*B*) data using the system model.

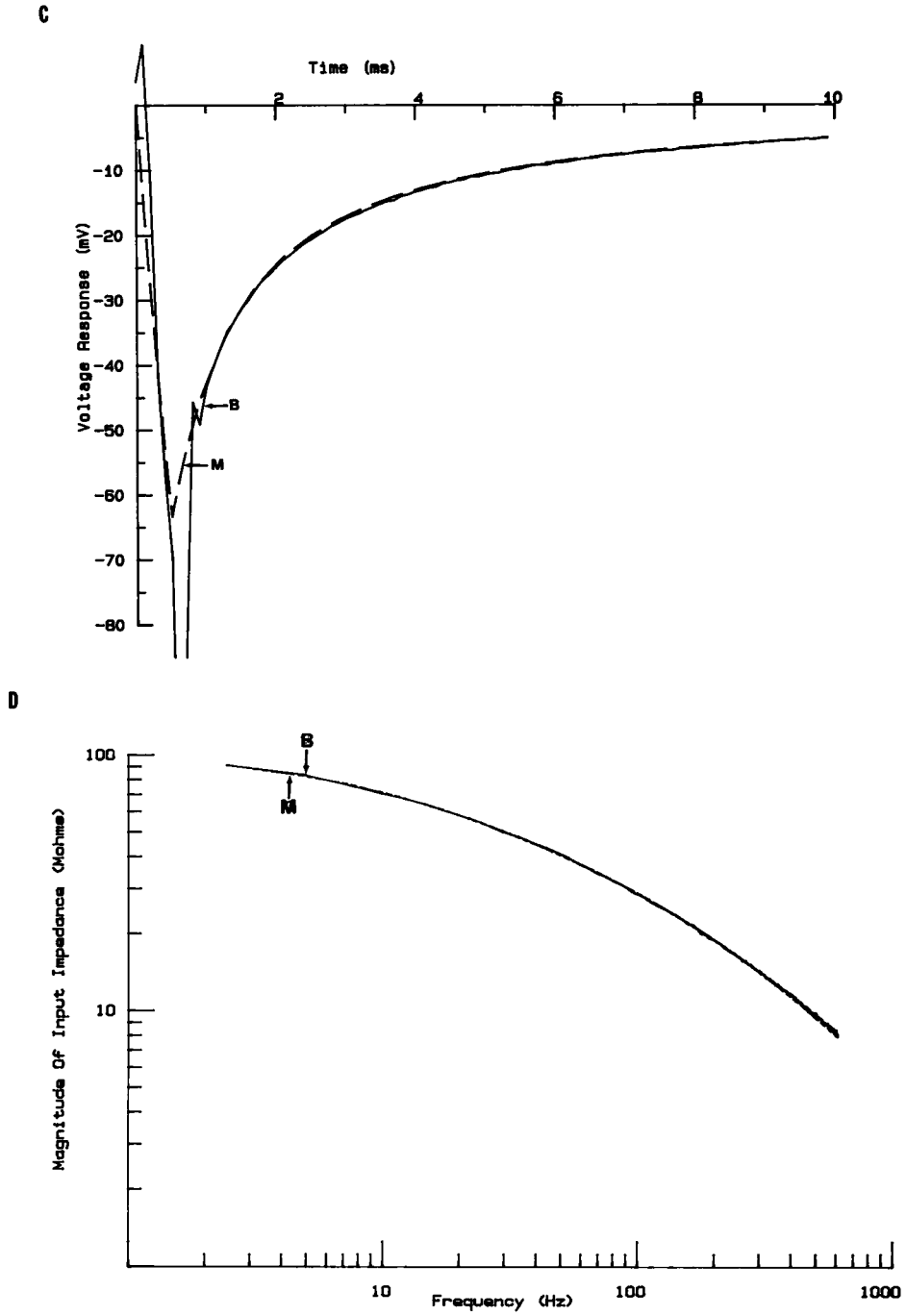

FIGURE 5 (*Continued*)

optimization strategy for estimating the system model parameters is a valid approach. However, it should be emphasized that such an optimization strategy leads to a local optimum which may or may not be the global optimum. Thus, uniqueness of the estimated parameters is not guaranteed, and different starting values for the model parameters should be used to check for optimality of the solution.

The application of the system and signal models to biological data from a dentate granule neuron demonstrated the advantages of the system model approach. Even though only one voltage response (Fig. 5 *a*) was

TABLE 3 Estimates of signal model parameters of a Dentate Granule Neuron

n	nth coefficient	nth time constant
	mV	*ms*
0	148.6	31.20
1	152.9	8.11
2	119.8	2.35
3	53.1	0.65

An optimization strategy was used to obtain the coefficients and time constants of a 50 ms, average voltage response to hyperpolarizing short current pulses (0.5 ms, 5 nA).

analyzed, the selected voltage response was similar to recordings from over 20 dentate granule neurons. The network elements and the specific membrane resistances and capacitances, estimated using the signal model approach were markedly different from those estimated using the system model approach. However, the input resistance estimates obtained from the two approaches differ by only 1.5%. Also, the specific membrane capacitance (~5 $\mu F/cm^2$) estimated using the system model approach is in agreement with that reported by Durand (8), but different from the generally accepted standard of 1 $\mu F/cm^2$. It should be noted that differences between modeled and biological data can be caused by a number of factors such as noise in the biological recordings, nonlinear properties of the electrode or the neuron, inaccurate measurements of the neuronal surface area, and errors caused by the choice of the ladder configuration.

The system model is more useful than the signal model for several reasons. (*a*) The signal model requires a current pulse for stimulation whereas the system model can use any stimulus which does not trigger system nonlinearities. The input impedance of a linear system is not dependent upon the type of stimulus used to elicit the voltage response. Therefore, choosing other forms of stimuli (i.e., triangular pulse, sinusoidal pulse) could minimize the artifacts caused by the square pulse stimulation. (*b*) The signal model requires estimation of time

TABLE 4 Estimates of system model parameters of a Dentate Granule Neuron

Parameter	System model estimate	Signal model estimate	Percentage difference
G_S (*nS*)	6.94	5.16	25.6
C_S (*pF*)	22.5	11.5	48.9
R_A ($M\Omega$)	13.9	4.89	64.8
G_M (*nS*)	0.272	0.103	62.1
C_M (*pF*)	11.3	4.24	62.8

System model estimates were obtained as described in section IV. The signal model estimates were obtained as described in reference 9 and using mean values of reported (8) morphological data (l_d = 287 μm, a = 1.2 μm, A_s = 470 μm^2).

TABLE 5 Estimates of specific resistances and capacitances of a dentate granule neuron using mean values of reported morphological data

Parameter	System model estimates	Signal model estimates
R_{ms} ($\Omega\ cm^2$)	677	911
R_{md} ($\Omega\ cm^2$)	6365	16807
R_i ($\Omega\ cm$)	438	154
C_{ms} ($\mu F/cm^2$)	4.79	2.45
C_{md} ($\mu F/cm^2$)	6.53	2.45

Data from reference 8: l_d = 287 μm, a = 1.2 μm, A_s = 470 μm^2. Reported (8) mean values for the signal model estimates are R_{ms} = 1,010 Ωcm^2, R_{md} = 6,632 Ωcm^2, R_i = 173.4 Ωcm, C_{ms} = 4.48 $\mu F/cm^2$, C_{md} = 4.48 $\mu F/cm^2$.

constants and coefficients of exponential terms, but practically only two or three terms can be reliably estimated from measured voltage responses to a current pulse. In comparison, a system model with 20 compartments would theoretically have 21 exponential terms in its signal model. (*c*) To determine the cable properties, from the signal model parameters, transcendental equations have to be solved using an iterative procedure (9). This further increases the estimation error. (*d*) For parameter estimation using an optimization strategy, the system model approach is more suitble than the signal model approach, because a significantly lower number of model parameters are used. For example, consider a uniform RC ladder network having 20 compartments; in the system model approach only five parameters are needed, whereas in the signal model approach, for the same degree of accuracy, 42 parameters (21 exponential terms) are needed. Furthermore, in the system model approach the network elements are estimated directy, whereas in the signal model approach transcendental equations still need to be solved (Appendix III and [9]) to obtain the network elements. (*e*) For parameter estimation, the most significant frequency components of the voltage response are, (*i*) the low-frequency components in the system model approach, and (*ii*) the high-frequency components (which are more susceptible to stimulus artifacts) in the signal model approach. Thus, the system model approach has better noise-handling performance for biological data.

In summary, this paper describes a system model approach for investigating the passive electrical properties of neurons. Such an approach has a sound theoretical foundation and can be practically applied to biological data.

APPENDIX I

The components of the gradient vector $\nabla|Z_i|^2$ are the partial derivatives of $|Z_i|^2$ with respect to the transformed parameters of the optimization

strategy (d_1, d_2, d_3, d_4, d_5). They are given by

$$\frac{\partial|Z_i|^2}{\partial d_1} = \frac{\partial|Z_i|^2}{\partial G_S} 2\mu_1 d_1 \quad \text{(I1)}$$

$$\frac{\partial|Z_i|^2}{\partial d_2} = \frac{\partial|Z_i|^2}{\partial C_S} 2\mu_2 d_2 \quad \text{(I2)}$$

$$\frac{\partial|Z_i|^2}{\partial d_3} = \frac{\partial|Z_i|^2}{\partial R_A} 2\mu_3 d_3 \quad \text{(I3)}$$

$$\frac{\partial|Z_i|^2}{\partial d_4} = \frac{\partial|Z_i|^2}{\partial G_M} 2\mu_4 d_4 \quad \text{(I4)}$$

$$\frac{\partial|Z_i|^2}{\partial d_5} = \frac{\partial|Z_i|^2}{\partial C_M} 2\mu_5 d_5, \quad \text{(I5)}$$

where $\mu_1, \ldots, \mu_5$ are the scaling factors,

$$\frac{\partial|Z_i|^2}{\partial G_S} = [-2Re(Z_i)]|Z_i|^2 \quad \text{(I6)}$$

$$\frac{\partial|Z_i|^2}{\partial C_S} = [2wIm(Z_i)]|Z_i|^2 \quad \text{(I7)}$$

$$\frac{\partial|Z_i|^2}{\partial R_A} = [Re\{(G_M + sC_M)(F_5)\} - Re\{(G_M + sC_M)(F_3)\}]|Z_i|^2 \quad \text{(I8)}$$

$$\frac{\partial|Z_i|^2}{\partial G_M} = (Re\{R_A F_5\} - Re\{R_A F_3\} - 2Re\{F_4\})|Z_i|^2 \quad \text{(I9)}$$

$$\frac{\partial|Z_i|^2}{\partial C_M} = w(Im\{R_A F_3\} + 2Im\{F_4\} - Im\{R_A F_5\})|Z_i|^2, \quad \text{(I10)}$$

and

$$X_N = (p)^N - (q)^N$$

$$Y_N = (p)^N + (p)^N$$

$$F_1 = (N+1)X_N - NX_{N-1} = [(N+1)Y_N - NY_{N-1}]\left[\frac{R_A(G_M + sC_M) + 2}{(p-q)}\right]$$

$$F_2 = NX_{N-1} + nY_{N-1}\left[\frac{R_A(G_M + sC_M) + 2}{(p-q)}\right]$$

$$F_3 = \frac{(G_S + sC_S)F_1 + (G_M + sC_M)F_2}{(p^{N+1} - q^{N+1})(G_S + sC_S) - [p^N - q^N][(G_S - G_M) + s(C_S - C_M)]}$$

$$F_4 = \frac{X_N}{(p^{N+1} - q^{N+1})(G_S + sC_S) - [p^N - q^N][(G_S - G_M) + s(C_S - C_M)]}$$

$$F_5 = \frac{F_1}{p^{N+1} - q^{N+1} - p^N + q^N}.$$

Re{·} denotes the real component of the complex argument, Im{·} denotes the imaginary component of the complex argument.

The relative change in $|Z_i|^2$ due to a relative change in an element value (i.e., sensitivity) is given by

$$S_x = \frac{\text{relative change in } |Z_i|^2}{\text{relative change in } x} = \left(\frac{\Delta|Z_i|^2}{|Z_i|^2}\right)\Big/\left(\frac{\Delta x}{x}\right). \quad \text{(I11)}$$

Hence,

$$S_x = \left(\frac{x}{|Z_i|^2}\right)\left(\frac{\partial|Z_i|^2}{\partial x}\right). \quad \text{(I12)}$$

Where S_x is the sensitivity of $|Z_i|^2$ with respect to x, and Δx is the incremental change in x.

APPENDIX II

Input impedance of a neuron with an eccentrically placed soma: Consider a structure with two ladders where the number of compartments is set to 15 in the distal tree and to 5 in the apical tree. Eq. 7 is generalized for each of the two ladders, as follows:

$$\mathbf{W}_{15} = \begin{bmatrix} H_{11} \\ H_{12} \end{bmatrix} V_{01} \quad \text{(II1)}$$

and

$$\mathbf{W}_5 = \begin{bmatrix} H_{21} \\ H_{22} \end{bmatrix} V_{02}. \quad \text{(II2)}$$

The voltage and current are expressed at the soma as follows:

$$\mathbf{W}_{soma} = \begin{bmatrix} H_{11} \\ H_{12} + H_{22}(H_{11}/H_{21}) \end{bmatrix} V_{01}, \quad \text{(II3)}$$

where V_{01} and V_{02} are the voltages at the far end of the first and second ladders, respectively, and

$$H_{11} = [p^{16} - q^{16} - p^{15} + q^{15}]/(p-q)$$
$$H_{12} = [(p^{15} - q^{15})(G_M + sC_M)]/(p-q)$$
$$H_{21} = [p^6 - q^6 - p^5 + q^5]/(p-q)$$
$$H_{22} = [(p^5 - q^5)(G_M + sC_M)]/(p-q).$$

The input impedance for the system model is

$$Z_i = \frac{H_{11}}{(G_S + sC_S)H_{11} + [H_{12} + H_{22}(H_{11}/H_{21})]}. \quad \text{(II4)}$$

APPENDIX III

The system model parameters can be estimated from the signal model parameters using the somatic shunt cable model (9) for neurons as follows.

(*a*) The electrotonic parameters of neurons (the dendritic membrane time constant, the ratio of the somatic-to-dendritic time constants, the ratio of the somatic-to-dendritic resistance, and the electrotonic length) are related to the signal model parameters (the amplitude coefficients

and time constants in a multiexponential representation of a voltage response), by a set of simultaneous equations including a transcendental equation as described in reference 9. From the signal model parameters, the electrotonic parameters can be numerically obtained using an iterative approach (which involves a computer-aided global search) to solve the transcendental equation, as described in reference 9.

(*b*) From the electrotonic parameters and morphological measurements, the specific membrane resistances and capacitances of a neuron (R_{ms}, R_{md}, R_i, C_{ms}, and C_{md}) can be directly obtained from a set of equations described in reference 8.

(*c*) The system model parameters (G_S, C_S, R_A, G_M, and C_M) can then be obtained from the specific resistances and capacitances using Eqs. (13, a–f).

The authors would like to thank Ping Fu and Larry Takeuchi for their technical assistance.

This work has been supported by the Natural Sciences and Engineering Research Council of Canada (NSERC) and the Medical Research Council of Canada (MRC).

Received for publication 26 May 1988 and in final form 15 February 1989.

REFERENCES

1. Bracewell, R. N. 1978. The Fourier Transform and Its Application. New York: McGraw-Hill Book Co., New York.
2. Brown, T. H., R. A. Fricke, and D. H. Perkel. 1981. Passive electrical constants in three classes of hippocampal neurons. *J. Neurophysiol.* 46:812–827.
3. Brown, T. H., D. H. Perkel, J. C. Norris, and J. H. Peacock. 1981. Electronic structure and specific membrane properties of mouse dorsal root ganglion neurons. *J. Neurophysiol.* 45:1–15.
4. Burke, R. E., and G. T. Ten Bruggencate. 1971. Electronic characteristics of alpha motoneurons of varying size. *J. Physiol. (Lond.).* 212:1–20.
5. Carlen, P. L., and D. Durand. 1981. Modelling the postsynaptic location and magnitude of tonic conductance changes resulting from neurotransmitter or drugs. *Neuroscience.* 6:839–846.
6. Carlen, P. L., R. Werman, and Y. Yaari. 1980. Postsynaptic conductance associated with presynaptic inhibition in cat lumbar motoneurons. *J. Physiol. (Lond.).* 298:539–556.
7. D'Aguanno, A., B. L. Bardakjian, and P. L. Carlen. 1986. Passive neuronal membrane parameters: comparison of optimization and peeling methods. *IEEE Trans. Biomed. Eng.* BME-33:1188–1196.
8. Durand, D., and P. L. Carlen. 1985. Electrotonic parameters of neurons following chronic ethanol consumption. *J. Neurophysiol.* 54:807–817.
9. Durand, D. 1984. The somatic shunt cable model for neurons. *Biophys. J.* 46:645–653.
10. Durand, D., P. L. Carlen, N. Gurevich, A. Ho, and H. Kunov. 1983. Electrotonic parameters of rat dentate granule cells measured using short pulses and HRP staining. *J. Neurophysiol.* 50:1080–1097.
11. Edwards, D. H., and B. Mulloney. 1984. Compartmental models of electrotonic structures and synaptic integration in an identified neurone. *J. Physiol. (Lond.).* 348:89–113.
12. Fletcher, R. 1970. A new approach to variable metric algorithms. *Comput. J.* 13:317–322.
13. Fletcher, R. 1980. Practical Methods of Optimization. Vol. 1. Unconstrained optimization. John Wiley & Sons, New York.
14. Fletcher, R. 1980. Practical Methods of Optimization. Vol. 2. Constrained Optimizations. John Wiley & sons, New York.
15. Guillemin, E. A. 1957. Synthesis of Passive Networks. John Wiley & Sons, New York.
16. Hyat, W. H., and J. E. Kemmerly. 1978. Engineering Circuit Analysis. McGraw-Hill Book Co., New York.
17. Iansek, R., and S. J. Redman. 1973. An analysis of the cable properties of spinal motoneurones using a brief intracellular current pulse. *J. Physiol. (Lond.).* 234:613–636.
18. Jack, J. J. B., and S. J. Redman. 1980. An electrical description of the motoneurone, and its application to the analysis of synaptic potentials. *J. Physiol. (Lond.).* 215:321–352.
19. Jack, J. J. B., D. Noble, and R. W. Tsien. 1975. Electric Currents Flow in Excitable Cells. Oxford University Press, London.
20. Kreyszig, E. 1976. Advanced Engineering Mathematics. John Wiley & Sons, New York.
21. Lux, H. D., and D. A. Pollen. 1966. Electrical constants of neurons in the motor cortex of the cat. *J. Neurophysiol.* 29:207–220.
22. Macgregor, R. J., and E. R. Lewis. 1977. Neuron Modeling. Plenum Publishing Corp., New York.
23. Merickel, M. B., S. B. Kater, and E. D. Eyman. 1977. Analysis of a network of electrically coupled neurons producing rhythmic activity in snail helisoma trivolvis. *IEEE Trans. Biomed. Eng.* BME-24:277–287.
24. Oppenheim, A. V., and R. W. Schafer. 1975. Digital Signal Processing. Prentice-Hall, Englewood Cliffs, NJ.
25. Perkel, D. H., and B. Mulloney. 1978. Calibrating compartmental model of neurons. *Am. J. Physiol.* 235:R93–R98.
26. Perkel, D. H., B. Mulloney, and R. W. Budelli. 1981. Quantitative methods for predicting neuronal behavior. *Neuroscience.* 6:823–827.
27. Pottala, E. W., T. R. Colburn, and D. R. Humphrey. 1973. A dendritic compartment model neuron. *IEEE Trans. Biomed. Eng.* BME-20:132–139.
28. Puil, E., B. Gimbarzevsky, and R. M. Miura. 1986. Quantification of membrane properties of trigeminal root ganglion neurons in guinea pigs. *J. Neurophysiol.* 55:995–1016.
29. Rabiner, L. R., and B. Gold. 1975. Theory and Application of Digital Signal Processing. Prentice-Hall, Englewood Cliffs, NJ.
30. Rall, W. 1977. Core conductor theory and cable properties of neurons. *In* Handbook of Physiology. The Nervous System. Vol. 1. American Physiological Society, Bethesda, MD. 39–97.
31. Rall, W. 1960. Membrane potential transients and membrane time constant of motoneurons. *Explor. Neurol.* 2:503–532.
32. Rall, W. 1969. Time constants and electronic length constants of membrane cylinders and neurons. *Biophys. J.* 9:1483–1508.
33. Rall, W., and J. Rinzel. 1973. Branch input resistance and steady attenuation for input to one branch of a dendritic neuron model. *Biophys. J.* 13:648–688.
34. Schwarz, R. J., and B. Friedland. 1965. Linear Systems. McGraw-Hill Book Co., New York.
35. Segev, I., J. W. Fleshman, J. P. Miller, and B. Bunow. 1985. Modeling the electrical behavior of anatomically complex neurons using a network analysis program. *Biol. Cybern.* 53:27–40.
36. Shelton, D. P. 1985. Membrane resistivity estimates for the Pur-

kinje neuron by means of a passive computer model, *Neuroscience.* 14:111–131.

37. Strang, G. 1976. Linear Algebra and Its Applications. Academic Press, Inc., New York.

38. Turner, D., and P. A., Schwartzkroin. 1980. Steady state electronic analysis of intracellular stained hippocampal neurons. *J. Neurophysiol.* 44:184–199.

39. Turner, D. A. 1984. Segmental cable evaluation of somatic transients in hippocampal neurons (ca_1, ca_3, and dentate). *Biophys. J.* 46:73–84.

40. Wilson, G. B., E. J. Vertatschitsch, S. K. Sarna, and S. M. Sims. 1984. Analysis of smooth muscle constants by pole-zero method. *IEEE Trans. Biomed. Eng.* BME-31:310–316.